Molecular Crystals and Liquid Crystals

ISSN: 1542-1406 (Print) 1563-5287 (Online) Journal homepage: http://www.tandfonline.com/loi/gmcl20

Pyromellitic Diimide-Benzodithiophene Copolymer for Polymer Solar Cells: Effect of Side Chain Length and Thiophene π-Bridge on Optical and Electronic Properties

Chunhua Luo, Zhitao Shen, Xiangjian Meng, Li Han, Shuo Sun, Tie Lin, Jinglan Sun, Hui Peng & Junhao Chu

To cite this article: Chunhua Luo, Zhitao Shen, Xiangjian Meng, Li Han, Shuo Sun, Tie Lin, Jinglan Sun, Hui Peng & Junhao Chu (2014) Pyromellitic Diimide-Benzodithiophene Copolymer for Polymer Solar Cells: Effect of Side Chain Length and Thiophene π-Bridge on Optical and Electronic Properties, Molecular Crystals and Liquid Crystals, 604:1, 151-163, DOI: 10.1080/15421406.2014.968082

To link to this article: http://dx.doi.org/10.1080/15421406.2014.968082

Published online: 15 Dec 2014.

Mol. Cryst. Liq. Cryst., Vol. 604: pp. 151–163, 2014

ISSN: 1542-1406 print/1563-5287 online
DOI: 10.1080/15421406.2014.968082

Pyromellitic Diimide-Benzodithiophene Copolymer for Polymer Solar Cells: Effect of Side Chain Length and Thiophene π-Bridge on Optical and Electronic Properties

CHUNHUA LUO,[1,*] ZHITAO SHEN,[2] XIANGJIAN MENG,[1] LI HAN,[1] SHUO SUN,[1] TIE LIN,[1] JINGLAN SUN,[1] HUI PENG,[*] AND JUNHAO CHU[1]

[1]National Laboratory for Infrared Physics, Shanghai Institute of Technical Physics, Chinese Academy of Science, Shanghai, China
[2]Key Laboratory of Polarized Materials and Devices, Ministry of Education, East China Normal University, Shanghai, China

Three donor-acceptor conjugated polymers were synthesized by combining electron donating benzodithiophene and electron accepting pyromellitic diimide. The relationship between structure and optical, electrochemical properties of the polymers were investigated. The results indicate that replacing the 2-ethylhexyl side chain with the longer 2-octyldodecyl side chain stabilized both the HOMO and LUMO level, and the insertion of thiophene π-bridge between pyromellitic diimide and benzodithiophene led to bathochromic-shifted and broader absorption. The polymers were used as donor materials to fabricate polymer solar cells. The highest open-circuit voltages reached 0.69 V and power conversion efficiencies reached 0.11%.

Keywords: Pyromellitic diimide; benzodithiophene; conjugated polymer; structure property relationship; polymer solar cell

Introduction

Polymer solar cells (PSCs) have been attracting an amount of interest because they can be fabricated by roll to roll printing techniques and are light weight, flexible and low cost [1, 2]. So far, the bulk heterojunction (BHJ) structure, in which a soluble fullerene derivative is usually used as the electron accepting material and a conjugated polymer is used as the electron donating material, is the most efficient architecture for PSCs. The power conversion efficiency of PSCs based on the BHJ structure has exceeded 10% [2, 3]. However, compared to traditional inorganic solar cell, the efficiency and stability of PSCs are still low which restricts their practical application. The design and synthesis of new

[*]Address correspondence to C. H. Luo, National Laboratory for Infrared Physics, Shanghai Institute of Technical Physics, Chinese Academy of Science, Shanghai, 200083, China, E-mail: chunhua_luo@hotmail.com; H. Peng, Key Laboratory of Polarized Materials and Devices, Ministry of Education, East China Normal University, Shanghai, 200241, China, E-mail: hpeng@ee.ecnu.edu.cn

Color versions of one or more of the figures in the article can be found online at www.tandfonline.com/gmcl.

conjugated polymer with low bandgap, high charge carriers' mobility, good environmental stability is highly desired for the development of PSCs [4]. The donor-acceptor approach by copolymerizing electron-deficient and electron-rich units to form donor-acceptor (D-A) conjugated polymers enables the manipulation of both the bandgap and energy level and is the most promising technique [5, 6].

Pyromellitic diimide (PMDI) belongs to the aromatic tetracarboxylic diimides which are regarded as promising n-type semiconductors due to their high electron affinity and electron mobility [7, 8], and good stability. Aromatic tetracarboxylic diimides are also good candidate for constructing D-A conjugated polymer as an electron deficient component. There have been a lot of reports on the synthesis and application of perylene diimide (PDI) and naphthalene diimide (NDI) based conjugated polymer in PSCs and organic field effect transistor [9–16]. However, compared to PDI and NDI, the use of PMDI based conjugated polymer in PSCs is rarely investigated. The copolymerization of PMDI with different electron donating unit can tune the bandgap and solubility of the resulting polymers. PMDI also has a modest LUMO energy level ($E_{LUMO} = \sim$–3.6 eV) [17] , so conjugated polymers based on PMDI have the potential to be used as acceptor materials in all polymer solar cells, or as donor materials in polymer-fullerene composite solar cells [18].

In this work, we report the synthesis, characterization and photovoltaic application of three D-A conjugated polymers based on PMDI and benzodithiophene (BDT). For comparison, two different alkyl side chain, 2-ethylhexyl and 2-octyldodecyl, were functionalized to the nitrogen atom in the PMDI unit, and a thiophene π-bridge was introduced between PMDI and BDT for the polymer P3. The solar cells were fabricated by using these PMDI based polymer as a donor and [6,6]-phenyl-C61-butyric acid methyl ester (PCBM) as an acceptor. The effect of active layer compositions and annealing temperatures on device performances were examined.

Materials and Methods

Materials

All chemicals were purchased from Aldrich, Alfa Aesar and other commercial resource and used as received. Tetrahydrofuran (THF) and toluene were distilled after drying with sodium/benzophenone. Acetic acid was refluxed with 2.5 % (w/w) $KMnO_4$ and 5 % (w/w) acetic anhydride under nitrogen for 4 hour and distilled before use. All Stille reactions were carried out under nitrogen atmosphere using standard Schlenk line techniques. 2-octyl-1-dodecylamine and 3,6-dibromopyromellitic dianhydride were synthesized according to the published procedure[17, 21][19, 20].

Characterization

Molecular weight measurement was performed on a Waters 515 GPC system using THF as the eluent, polystyrene as standard and a Waters RI detector at 35°C. UV-vis absorptions were recorded on a Persee TU-1901 UV-Visible spectrometer. Cyclic voltammetry (CV) was performed on a Metrohm Autolab Aut 85013 Electrochemical Workstation in 0.2 mol/L of $LiClO_4$ acetonitrile solution. A glass carbon electrode coated with a thin layer of the polymer, a Pt wire, and a Ag/AgCl electrode were used as the working electrode, counter electrode and reference electrode, respectively. The CV curves were calibrated by using the ferrocene/ferrocenium (Fc/Fc+) redox couple as an external standard which was measured under same conditions before and after the measurement of samples. Thermogravimetric measurements were performed on a STA449F3 thermogravimetric

analyzer from Netzsch instruments. The sample was heated from ambient to 600°C at a heating rate of 10°C min^{-1} under an inert atmosphere of nitrogen. Differential scanning calorimetry (DSC) experiments were carried out by using a Perkin-Elmer DSC-7 instrument and samples were purged with dry nitrogen at a ramping rate of 10°C min^{-1}.

Solar Cell Fabrication and Characterization

Polymer solar cells (PSCs) were fabricated with a structure of ITO/ PEDOT:PSS/Polymer:PCBM/LiF/Al on commercial ITO-coated glass substrate (the surface resistance of ca. 20 Ω $square^{-1}$). The ITO glass substrates were cleaned in an ultrasonic bath in detergent, D.I. water, acetone and isopropyl alcohol each for 15 min. A thin layer (40 nm) of PEDOT:PSS (poly(3,4-ethylenedioxythiophene)- poly(styrene sulfonate)) was spin-coated (3500 rpm, 30 s) on the ITO substrate and dried at 90°C for 30 min in a vacuum oven. Subsequently, the photosensitive active layer (80 nm) was prepared on the top of the PEDOT:PSS layer by spin coating (1000 rpm, 15s) from the composite solutions (polymer/PCBM with a total concentration of 15 mg mL^{-1} in chloroform). The resulting film was annealed at 110°C or 150°C for 15 min in a vacuum oven. The device was completed by thermal evaporating a thin layer of LiF (1 nm) and an aluminum cathode (∼150 nm) on the active layer under a shadow mask. The active area of the devices was 4 × 4 mm^2 or 5 × 5 mm^2 defined by the mask. The current-voltage (J–V) curves were measured under simulated AM 1.5G irradiation (100 mW cm^{-2}) by using an Abet technologies sun 2000 solar simulator. All cells were prepared and measured under ambient conditions.

Synthesis of Monomers and Polymers

3,6-dibromopyromellitic dianhydride. 3,6-dibromopyromellitic dianhydride was synthesized from tetramethylbenzene through three steps reaction according to the published procedure[17, 21]. ^{1}H NMR (400 MHz, DMSO-d6, δ): no signals. ^{13}C NMR (300 MHz, DMSO-d6, δ): 158.54, 137.33, 115.32.

3,6-dibromo-N,N'-(2-ethylhexyl)- pyromellitic diimide (M1). To a three-neck flask equipped with a nitrogen inlet and a dropping funnel were added the compound **4** (2.4 g, 6.38 mmol), glacial acetic acid (30 mL) and 2-ethylhexylamine (2.61 mL, 15.96 mmol). The reaction solution was refluxed overnight. After reaction, the mixture was concentrated under reduced pressure. Then methanol (50 mL) was added and the precipitate was collected by the filtration. The crude product was purified by the column chromatography (silica gel, dichloromethane: hexane 3:1) to give a colorless solid (3.15 g, 82 %). ^{1}H NMR (400MHz, CDCl3, δ): 3.55 (d, 4H), 1.77(m, 2H), 1.24 (m, 16H), 0.83 (m, 12H). ^{13}C NMR(300 MHz, CDCl3, δ): 163.28, 135.65, 113.63, 42.42, 37.75, 30.07, 28.02, 23.43, 22.45,13.56, 9.89.

3,6-dibromo-N,N'-(2-octyldodecyl)- pyromellitic diimide (M2). 3,6-dibromo-N,N'-(2-octyldodecyl)-pyromellitic diimide was synthesized used the same method as M1. After purification of the crude product by the column chromatography, a light yellow solid was obtained (Yield = 79 %). ^{1}H NMR (400MHz, CDCl3, δ): 3.60 (d, 4H), 1.86(m, 2H), 1.24 (m, 64H), 0.87 (m, 12H). ^{13}C NMR(300 MHz, CDCl3, δ): 163.67, 136.07, 114.05, 43.28, 36.88, 31.89, 31.85 , 31.44, 29.87, 29.59, 29.55, 29.50, 29.32, 29.25, 26.22, 22.66, 22.64, 14.09.

3,6-bis(thiophen-2-yl)-N,N'-(2-octyldodecyl)-pyromellitic diimide (5). To a three neck Schlenk flask was added M2 (935 mg, 1.0 mmol), tris(dibenzylideneacetone)dipalladium(0)

($Pd_2(dba)_3$) (45.6 mg) and tri(*o*-tolyl)phosphine (P(*o*-tol)$_3$) (60 mg). The flask was subjected to three cycles of evacuation and addition of nitrogen. Then 30 ml toluene and 2-(tributylstannyl)thiophene (2.5 mmol, 934 mg) were injected into the flask under vigorous stirring. The reaction mixture was stirred overnight at 80 °C under nitrogen. After the reaction, the solvent was removed under reduced pressure and the solid was purified by silica chromatography with dichloromethane: hexane = 1: 1 as the eluent to afford the compound 5 as bright yellow solid (929 mg, yield = 98.7 %). ^{1}H NMR (400MHz, aceton-d6, δ): 7.72 (q, 2H), 7.27 (q, 2H), 7.18 (q, 2H), 3.45 (d, 4H), 1.80(m, 2H), 1.25 (m, 64H), 0.86 (m, 12H).

3,6-bis(5-bromothiophen-2-yl)-N,N'-(2-octyldedocyl)-pyromellitic diimide (M3). To a three neck flask equipped with a dropping funnel were added the compound **5** (0.5 mmol, 470.7 mg) 5, 5 mL chloroform and 1mL 40 % aqueous hydrobromic acid. A mixture of bromine and 40 % aqueous hydrobromic acid (1:1, v/v) was added dropwise under vigorous stirring at 50 °C and the reaction was monitored by TLC. After the disappearance of the starting material, the reaction solution was cooled to room temperature then poured into water. The mixture was extracted with chloroform (3×15 mL). The organic phase was combined, washed with 10 % sodium thiosulfate solution (15 mL×2) and water (2×20 mL), and dried (Mg_2SO_4). Then solvent was removed under reduced pressure to give yellow crude product. The crude product was purified by column chromatography on silica gel (hexane/dichloromethane, 1:1) to give the title compound as yellow solid (yield = 82.4 %). ^{1}H NMR (400MHz, aceton-d6, δ): 7.25 (d, 2H), 7.12 (d, 2H), 3.50 (d, 4H), 1.82 (m, 2H), 1.26 (m, 64H), 0.86 (m, 12H). ^{13}C NMR(300 MHz, CDCl3, δ): 164.76, 135.18, 130.94, 130.65, 129.77, 129.61, 115.51, 43.98, 36.76, 31.86, 31.82, 31.42, 29.91, 29.57, 29.49, 29.43, 29.29, 29.23, 26.12, 22.63, 14.07.

Synthesis of the polymer P1

The dibromopyromellitic diimide monomer M1 (180 mg, 1 equiv.), bis(trimethylstannyl) comonomer 1,1'-[4,8-bis[(2-ethylhexyl)oxy]benzo[1,2-b:4,5-b']dithiophene-2,6-diyl]bis[1,1,1-trimethylstannane] (BDT, 232 mg, 1 equiv), $Pd_2(dba)_3$ (9.0 mg, 5 mol %.) and P(*o*-tol)$_3$ (18 mg, 16 mol %) were added into a Schlenk flask which was subjected to three cycles of evacuation and admission of nitrogen. Then 25 mL of toluene was injected into the flask and the reaction mixture was stirred at 100°C for 48 hours. After the reaction, the reaction solution was concentrated and precipitated into 100 mL of methanol. The precipitate was filtered and purified via Soxhlet extraction with methanol for 24 h and with hexane for 24 h, then extracted with chloroform until the extracted solution appeared colorless. The chloroform solution was pass through a 4–5 cm celite 545 column and then collected. The chloroform solution was concentrated by evaporation of solvent and precipitated into methanol (200 mL) and filtered to afford a dark red solid (232 mg, yield = 87 %).

Synthesis of the polymer P2

The polymer P2 was synthesized by the same procedure as that of P1 using 281 mg of M2 and 232 mg BDT. A dark red solid was obtained (345 mg, yield = 94 %).

Synthesis of polymer P3

The polymer P3 was synthesized by the same method as that of P1 using 220 mg of M3 and 155 mg BDT. After precipitating of the chloroform solution into methanol, a dark red solid was obtained (241 mg, yield = 87 %)

Results and Discussion

Synthesis and Characterization of Polymers

The PMDI based monomer M1 and M2 (Scheme 1) were synthesized in accordance with the procedure reported in the literature [17, 21]. The yield was 82 % for monomer M1 and 79 % for M2. M3 was synthesized from M2 through two steps reaction. Stille coupling of monomer M2 with 2-(tributylstannyl)thiophene give the 3,6-bis(thiophen-2-yl)-N,N'-(2-octyl)dodecylamine)-pyromellitic diimide (yield = 99%), which was brominated by bromine/hydrobromic acid to afford the monomer M3 in 82 % yield.

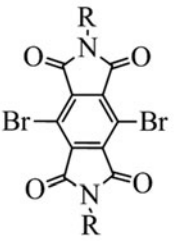

M1 R = 2-ethylhexyl

M2 R = 2-octyldodecyl

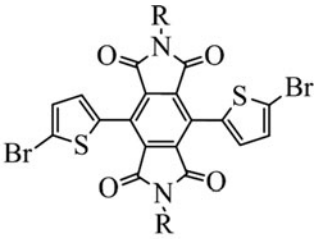

M3 R = 2-octyldodecyl

Scheme 1. Chemical structure of PMDI based monomers M1, M2 and M3.

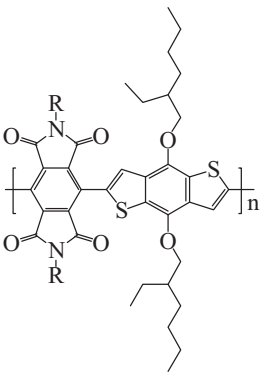

P1 R=$CH_2CH(C_2H_5)C_4H_9$

P2 R= $CH_2CH(C_8H_{17})C_{10}H_{21}$

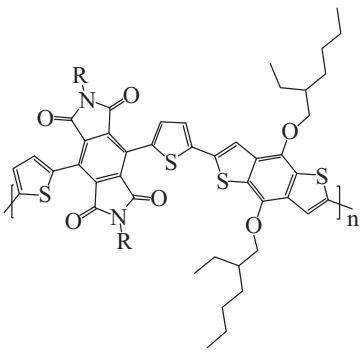

P3 R= $CH_2CH(C_8H_{17})C_{10}H_{21}$

Scheme 2. Chemical structure of polymers P1-P3.

PMDI-based polymers P1-P3 (Scheme 2) were synthesized from dibromopyromellitic diimide monomers with bis(trimethylstannyl) benzodithiophene comonomer via Pd-catalyzed Stille coupling. Table 1 lists the product yields and the molecular weights of the synthesized polymers. The yields of the three polymers are all over 87 %. The number average molecular weight ($M_{n)}$ is in the range of 23∼66 KDa and the polydispersity is between 2.0 and 3. The polymers are soluble in common organic solvents, such as dichloromethane, chloroform, THF, toluene and chlorobenzene. The chemical structure of polymers was

Table 1. Product yields, molecular weight distribution, thermal properties, optical properties and electrochemical data for polymers P1-P3

Polymer	Yield (%)	M_n[a] (KDa)	M_w/M_n	T_d (°C)	T_g (°C)	$\lambda_{max\ (soln,nm)}$	$\lambda_{max\ (film,nm)}$	$\lambda_{onset\ (film,nm)}$	E_g^{opt} (ev)	[b]E_{HOMO} (ev)	[c]E_{LUMO} (ev)
P1	87	50.7	2.52	325	—	436	433	536	2.31	−5.70	−3.39
P2	94	23.2	2.84	337	163	435	476	576	2.15	−5.82	−3.67
P3	87	66.2	2.01	342	—	452	460	558	2.22	−5.84	−3.62

[a]Molecular weight distribution were determined by GPC using THF as the eluent and polystyrene as standard; [b]calculated from the onset oxidation peaks based on the equation: $E_{HOMO} = -(E_{ox}^{onset} + 4.4)$ ev; [c]calculated based on equation: $E_{LUMO} = E_{HOMO} + E_g^{opt}$

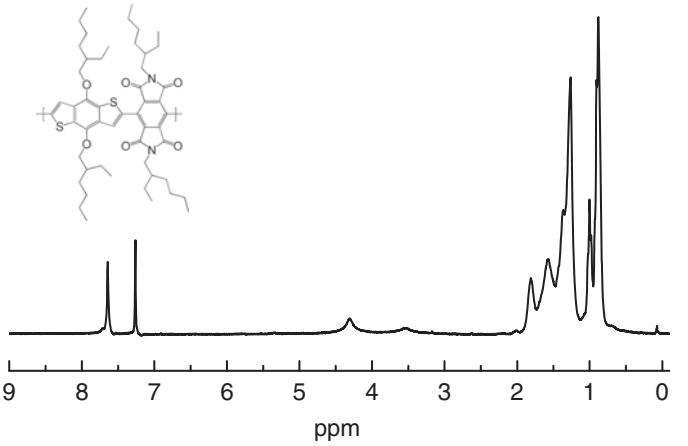

Figure 1. ^{1}H NMR spectra of polymer P1 in $CDCl_3$.

characterized by proton NMR (Figures 1–3). In the ^{1}H NMR spectra of polymers P1∼P3, signals between 0.8–4 ppm are assigned to alkyl side-chain protons in both the PMDI and the BDT units and signals observed between 7–8 ppm are corresponding to aromatic protons of the donor unit.

The results of thermogravimetric analysis (TGA) are give in Figure 4 and summarized in Table 1. It can be seen that the thermal decomposition temperatures (T_d) of these copolymers were above 300°C, which demonstrate that the thermal stability of these PMDI-based polymers is good enough for their applications in OPV and other optoelectronic devices. Figure 5 give the results of differential scanning calorimetry (DSC) analysis. No thermal transition was observed for the polymers P1 and P3 up to 300°C. However, on heating, an endothermic peak was found at 163°C for the polymer P2 but no obvious exothermic feature was detected on cooling. In the second heating / cooling cycle, the

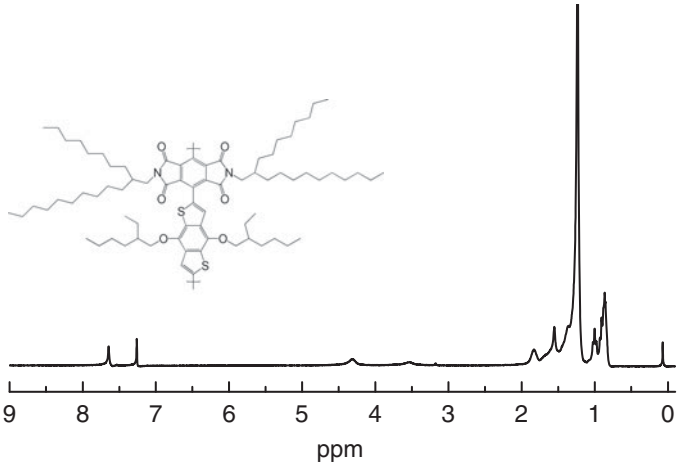

Figure 2. ^{1}H NMR spectra of polymer P2 in $CDCl_3$.

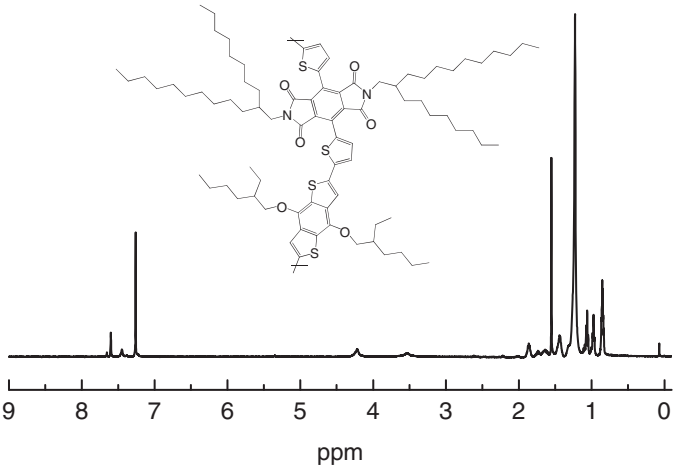

Figure 3. ^{1}H NMR spectra of polymer P3 in $CDCl_3$.

behavior was the same (Figure 5). The absence of exothermic feature on the cooling process could be due to the slow crystallization of P2 which could not be detected.

Optical Properties

The UV-vis absorption spectra of P1-P3 in a chloroform solution and as solid thin film on a quartz substrate are represented in Figure 6, and the photophysical data are also summarized in Table 1. In the solution, the absorption profiles of P1 and P2 are very similar and contain two major absorption bands. One is in the ultraviolet region (320 nm) with a shoulder at 348 nm and the other is in the visible region centered at 435 nm. The absorption band at 534 nm should be associated to the intramolecular donor-acceptor

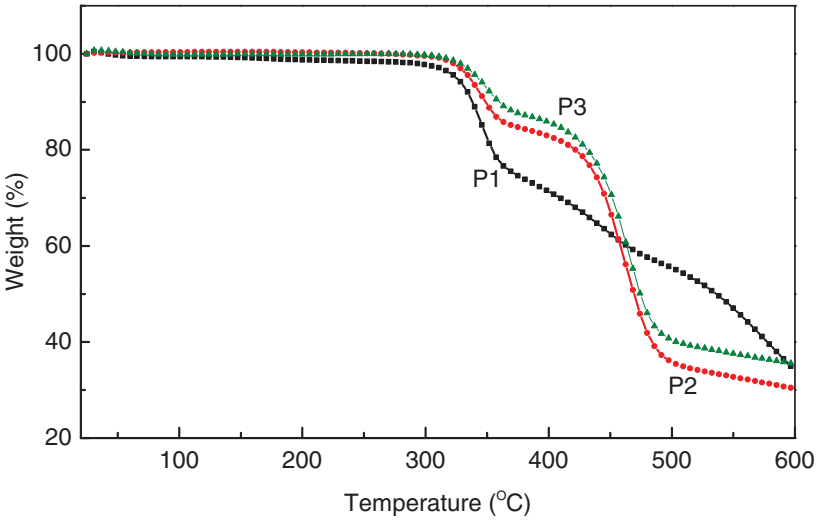

Figure 4. TGA thermograms of PMDI polymers: (a) P1; (b) P2; (c) P3.

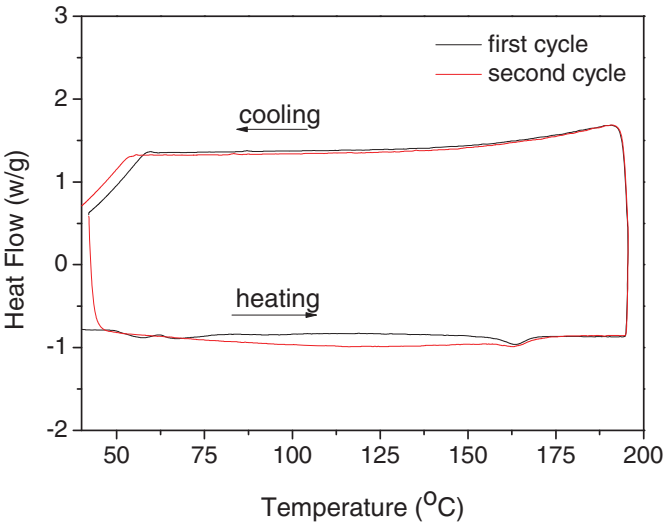

Figure 5. DSC thermogram for polymer P2.

charge-transfer (ICT) interaction [22, 23]. Compared to P1 and P2, the polymer P3 which has a thiophene π-bridge between PMDI and the BDT units exhibits higher intensity for the ICT transition. P3 also shows broader and bathochromic-shifted absorption in contrast to P2. This is reasonable. Because the insertion of a thiophene π-bridge between PMDI and the electron donating unit can decrease the intramolecular steric hidrance and improve the molecular coplanarity and conjugation of the polymer. In the solid film state, the absorption profile of P1 is similar to that of its solution. While, the adsorption bands of the P2 film are largely red-shifted (41 nm). This suggested strong intermolecular π–π packing and

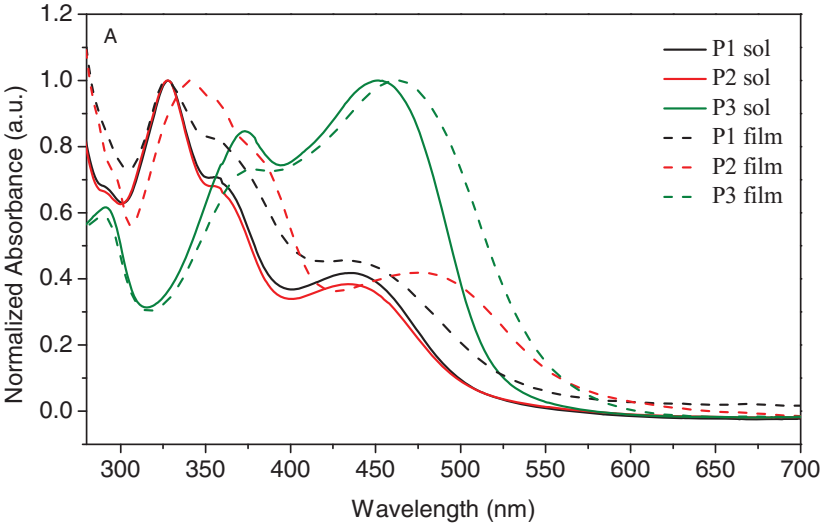

Figure 6. Normalized UV–vis absorption spectra of polymers P1-P3 in $CHCl_3$ solution and as thin film on quartz substrate.

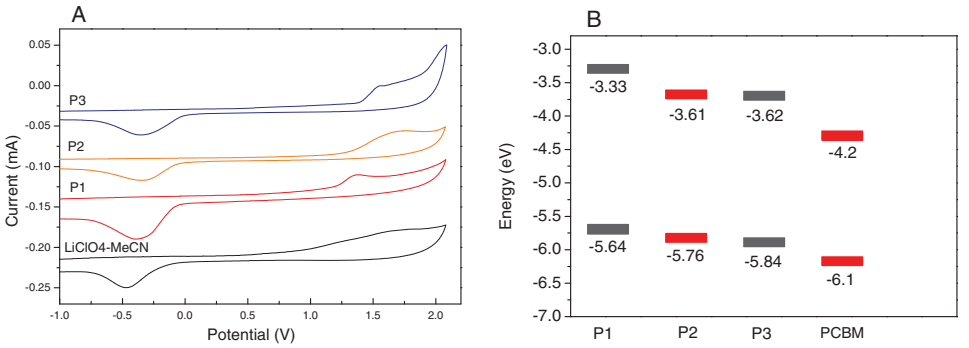

Figure 7. Cyclic voltammograms of films for polymers P1-P3 on glass carbon plate in an acetonitrile solution of 0.2 M LiClO4 with a potential scan rate of 50 mV/s (A); and (B) The HOMO and LUMO energy levels for P1-P3.

ordered arrangement of polymer chains could exist in P2, which was also supported by the observation of crystallization transition in DSC. The optical bandgaps, estimated from the low-energy absorption onset wavelength ($E_g^{opt} = 1240\ \lambda_{onset}^{-1}$) were 2.31 eV for P1, 2.22 eV for P3, 2.15 eV for P2.

Electrochemical Characterization

Cyclic voltammetry (CV) experiments were carried out to study the electrochemical redox properties and estimate the HOMO and LUMO energy levels of the polymers P1-P3. CV was performed on the thin films of the polymer. The obtained voltammograms are shown in Figure 7. The CV curves show one or two oxidation peaks appeared between 1.0 V∼1.7 V, and no obvious reduction peaks was observed for any of the three PMDI-based polymers in the negative scan. These results indicate that these PMDI based polymers are more likely to be p-type materials.

The HOMO energy levels were estimated from the onset oxidation poteatials ((E_{ox}^{onset}). The reference electrode was calibrated with ferrocene ($E_{ferrocene}^{1/2} = 0.40V\ vs\ Ag/AgCl$). The HOMO energy levels of the polymers were then calculated from the onset oxidation potentials) according to the equation: $E_{HOMO} = -(E_{ox}^{onset} + 4.4)$ ev[24], where E_{ox}^{onset} is the

Table 2. Photovoltaic properties of the polymer solar cells under AM 1.5 G illumination at 100 mW cm^{-2}

Polymer :PCBM (w/w)	Pre-annealing	V_{oc} (V)	J_{sc} (mA/cm^2)	FF (%)	PCE (%)
P1 :PCBM (1:2)	no	0.48	0.693	29	0.089
P2 :PCBM (1:2)	no	0.56	0.273	19	0.029
P3 :PCBM (1:1)	no	0.69	0.678	24	0.11

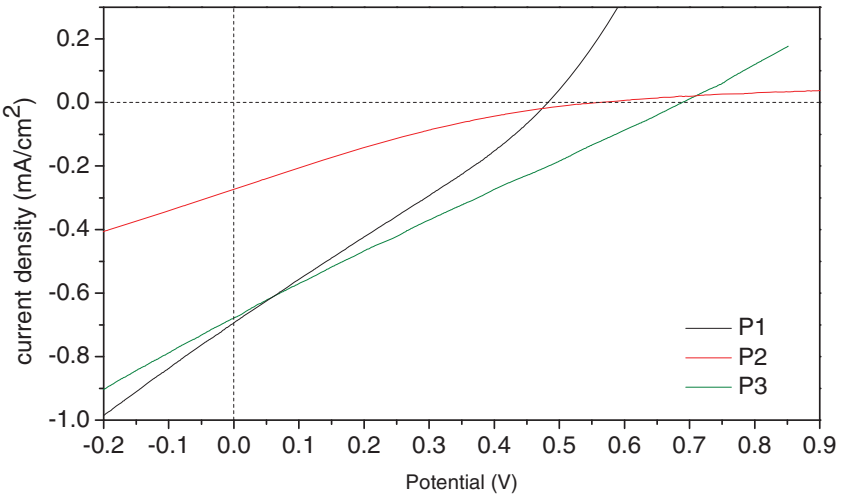

Figure 8. J-V curve of PMDI-based polymer solar cells with active layer composition of P: PCBM (1:2, w/w) for P1-P2, P3: PCBM (1:1, w/w) under illumination of AM 1.5 G, 100 mW/cm^2.

measured potential relative to the Ag/AgCl reference electrode. The LUMO energy level was calculated from the optical band gap and the HOMO energy level according to the following equation: $E_{LUMO} = E_{HOMO} + E_g{}^{opt}$, where $E_g{}^{opt}$ is the optical band gap obtained from the UV-Vis spectra. The HOMO and LUMO energy levels are listed in Table 1. The HOMO and LUMO energy of P2 are deeper compared to P1, indicated that the replacing of 2-ethylhexyl side chain with 2-octyldodecyl can stabilize both of the HOMO and LUMO energy level. The relatively low lying HOMO energy level of P3 compared to the others suggests a higher open circuit potential could be obtained for P3 when it is used as the donor material in polymer/PCBM solar cell.

Solar Cell Performance

The polymer solar cells with a device structure of glass/ITO /PEDOT:PSS /Polymer:PCBM/LiF/Al were fabricated by using the PMDI based polymer as the electron donor and PCBM as the electron acceptor. The weight ratio of the polymer to PCBM was varied from 2:1, 1:1 to 1:2 to optimize the active layer composition. The best device performance were achieved with a 1:2 donor/acceptor weight ratio for the polymers P1 and P2, and a 1:1 weight ratio for the polymer P3. The effect of pre-thermal annealing on solar cell performance was also studied by thermal treatment of the active layer compositions at 110°C or 150°C before LiF and Al deposition. For P1, the PCE increased with increasing annealing temperature and the best performance was obtained with the active layer annealed at 150°C. The enhancement of PCE results from the increasing V_{oc}. On the contrary, the PCEs of P3 reduced when the thermal annealing temperature increased. The PCE of P2 was first improved after the active layer annealed at 110°C then drastically declined with the cell annealed at 150°C. The highest open circuit voltage of 0.69 V was obtained for the polymer 3 with a power conversion efficiency of 0.11%.

A representative current density–voltage (J–V) curves of the prepared PSCs under the illumination of AM 1.5 G, 100 mW cm^{-2} was shown in Figure 8 and the photovoltaic performance data of the PSCs, including the open circuit voltage (V_{oc}), short circuit current

density (J_{sc}), fill factor (FF), and power conversion efficiency (PCE) values, are summarized in Table 2. The results shows that although polymer P2 has relatively narrow bandgaps, the polymer solar cells based on P1 display much higher J_{sc} than P2. This again confirm that bulky side chain could reduce the miscibility of conjugated polymer with PCBM, resulting in the worse photovoltaic performance [25]. The PSC based on P3 show the best performance due to the low lying HOMO energy level, which contributed to the higher V_{oc}.

Conclusion

In conclusion, three D-A conjugated polymers based on pyromellitic diimide were synthesized by Stille-cross coupling with a high yield. These polymers exhibit good solubility in common organic solvents, high thermal stability and low-lying HOMO energy levels between $-5.70 \sim -5.85$ eV. The polymer P2 functioned with the long, bulkier 2-octyldodecyl side chain displays bath-chromic absorption and deeper HOMO and LUMO energy level in contrasted to the 2-ethylhexyl functioned polymer P1. Photovoltaic study using these PMDI based polymer as donor and PCBM as acceptor showed that the polymer bearing the shorter 2-ethyhexyl side chain has higher J_{sc} and FF compared to the polymer with 2-octyldodecyl side chain. The insertion of a thiophene π-bridge between PMDI and electron donor unit decreased the intramolecular steric hindrance and resulted in broader absorption and improved photovoltaic performance.

Funding

This work was financially supported by National Program on Key Basic Research project (973 Project, No. 2013CB922302), National Natural Science Foundation of China (No. 61306020), China Postdoctoral Science Foundation (NO. 2012M510897) and NCET

References

[1] Spanggaard, H., & Krebs, F. C. (2004). *Sol. Energy Mater. Sol. Cells*, *83*, 125.
[2] Su, Y.-W., Lan, S.-C., & Wei, K.-H. (2012). *Mater. Today*, *15*, 554.
[3] Scharber, M. C., & Sariciftci, N. S. (2013). *Prog. Polym. Sci.*, *38*, 1929.
[4] Dimitrov, S. D., & Durrant, J. R. *Chem. Mater.*, DOI: 10.1021/cm402403z
[5] Van Mullekom, H. A. M., Vekemans, J. A. J. M., Havinga, E. E., & Meijer, E. W. (2001). *Mater. Sci. Eng., R*, *32*, 1.
[6] Boudreault, P.-L. T., Najari, A., & Leclerc, M. (2010). *Chem. Mater.*, *23*, 456.
[7] Zhan, X., Facchetti, A., Barlow, S., Marks, T. J., Ratner, M. A., Wasielewski, M. R., & Marder, S. R. (2011). *Adv. Mater.*, *23*, 268.
[8] Li, C., & Wonneberger, H. (2012). *Adv. Mater.*, *24*, 613.
[9] Zhang, L., Di, C.-a., Zhao, Y., Guo, Y., Sun, X., Wen, Y., Zhou, W., Zhan, X., Yu, G., & Liu, Y. (2010). *Adv. Mater.*, *22*, 3537.
[10] Yan, H., Chen, Z., Zheng, Y., Newman, C., Quinn, J. R., Dotz, F., Kastler, M., & Facchetti A. (2009). *Nature*, *457*, 679.
[11] Zhou, E., Cong, J., Wei, Q., Tajima, K., Yang, C., & Hashimoto, K. (2011). *Angew. Chem., Int. Ed.*, *50*, 2799.
[12] Zhou, E., Cong, J., Zhao, M., Zhang, L., Hashimoto, K., & Tajima, K. (2012). *Chem. Commun.*, *48*, 5283.
[13] Hwang, Y.-J., Ren, G., Murari, N. M., & Jenekhe, S. A. (2012). *Macromolecules*, *45*, 9056.
[14] Hu, X., Zuo, L., Pan, H., Hao, F., Pan, J., Fu, L., Shi, M., & Chen, H. (2012). *Sol. Energy Mater. Sol. Cells*, *103*, 157.

[15] Yuan, M., Durban, M. M., Kazarinoff, P. D., Zeigler, D. F., Rice, A. H., Segawa, Y., & Luscombe, C. K. (2013) *J. Polym. Sci., Part A: Polym. Chem.*, *51*, 4061.
[16] Kim, R., Amegadze, P. S. K., Kang, I., Yun, H.-J., Noh, Y.-Y., Kwon, S.-K., & Kim, Y.-H. *Adv. Funct. Mater*. doi: 10.1002/adfm.201301197
[17] Guo, X., & Watson, M. D. (2011). *Macromolecules*, *44*, 6711.
[18] Yang, S., Zhang, W., Shen, X.-x., Liu, Y., Du, X.-y., Chen, S., Xiao, Z., Yang, Z.-y., Zuo, Q.-q., & Ding, L.-m. (2012). *Gaofenzi Xuebao*, *8*, 838.
[19] Guo, X., & Watson, M. D. (2008). *Org. Lett.*, *10*, 5333.
[20] Letizia, J. A., Salata, M. R., Tribout, C. M., Facchetti, A., Ratner, M. A., & Marks, T. J. (2008). *J. Am. Chem. Soc.*, *130*, 9679.
[21] Rhee, T. H., Choi, T., Chung, E. Y., & Suh, D. H. (2001). *Macromol. Chem. Phys.*, *202*, 906.
[22] Ghosh, S., & Ramakrishnan, S. (2004). *Angew. Chem. Int. Ed.*, *43*, 3264.
[23] Kato, S.-i., Matsumoto, T., Ideta, K., Shimasaki, T., Goto, K., & Shinmyozu, T. (2006). *J. Org. Chem.*, *71*, 4723.
[24] Wang, K., Jiang, P., Zhang, Z.-G., Fu, Q., & Li, Y. (2013). *Macromol. Chem. Phys.*, *214*, 1772.
[25] Palma, C.-A., Bjork, J., Bonini, M., Dyer, M. S., Llanes-Pallas, A., Bonifazi, D., Persson, M., & Samori, P. (2009). *J. Am. Chem. Soc.*, *131*, 13062.